THE RISE & FALL OF CRUSTAL POROSITY: INSIGHT ON EARLY MARTIAN HISTORY. S. Gyalay[1], F. Nimmo[1], A.-C. Plesa[2], M.A. Wieczorek[3], R. Citron[4,5], and G.S. Collins[6], [1]University of California, Santa Cruz (UCSC; Santa Cruz, CA 95060, USA; sgyalay@ucsc.edu), [2]German Aerospace Center (DLR; Berlin, Germany), [3]Institut de Physique du Globe de Paris (IPGP), Paris Cité, French National Centre for Scientific Research (Paris, 75005 France), [4]Massachusetts Institute of Technology (MIT; Cambridge, MA 02139, USA), [5]NASA Goddard Space Flight Center (Greenbelt, MD 20771, USA), [6]Imperial College London (London, UK).

Introduction: Beneath the late InSight Mars lander, the seismic wave speed at depth sharply increases at two intra-crustal boundaries [1-5]. This indicates the crust below InSight contains three separate layers with distinct compositions and/or porosities (detailed in Table 1). Differences in composition might suggest differences in the timing or mechanism behind each layer's formation, while differences in porosity may arise from the closure or generation of porosity at depth. We focus on the latter and ask what the depth of such porosity transitions would suggest about early Martian history—namely by investigating the closure of porosity through viscous creep and the generation of porosity by impact-induced tensile fragmentation.

z [5] (km)	V_S [5] (km/s)	Inferred composition, φ [6, 7]
8.5±1.5	~1.8	Fractured basalt and (cemented) sediments, φ=0.1-0.5
22±3	~2.6	(cemented) fractured basalts, φ=0.1-0.23; or more-felsic plagioclase feldspar, φ=0.0-0.23
43±5	~3.6	Competent rock, φ=0
	~4.0	Mantle, φ=0

Table 1: For each layer in the Martian crust, we list the depth z at its base, its shear wave velocity V_S, its inferred composition, and its porosity φ.

Viscous Pore Closure: The early Martian crust was thoroughly fractured by large impacts [8]. Further, early Mars was warm from the heat of accretion and abundant radionuclides [e.g. 9, 10]. Thus, like chocolate chips in a double boiler, the viscosity of hotter fragments lowered until the rock flowed—closing pore spaces between fragments. The pore closure rate depends exponentially on the rock's viscosity, which itself has an exponential dependence on temperature. Because temperature increases with depth, a sharp contrast would form between shallow, cold, porous rock and deep, warm, solid rock. The exact depth of this transition depends on the thermal gradient (and thus heat flow) when this viscous pore closure occurred. Having cooled since then, the depth of this intracrustal boundary would be a fossil of how hot Mars was when porosity was last significantly generated.

In previous work [11], we linked the evolution of crustal porosity structure [e.g. 12] to thermal evolution models of Mars [10]. If any detected discontinuities in seismic wave speed are indeed due to pore closure, we can thus estimate the latest each would occur (Figure 1). We concluded that if the shallower discontinuity in seismic wave speed at 8.5 km depth was due to pore closure, the closure aligned temporally with when we expect the last large-basin-forming impacts to have occurred on Mars [11]. However, later observations of a second, deeper intracrustal boundary at a depth of 22 km [2-4] and porosity between the two boundaries [7, 13] complicated the matter.

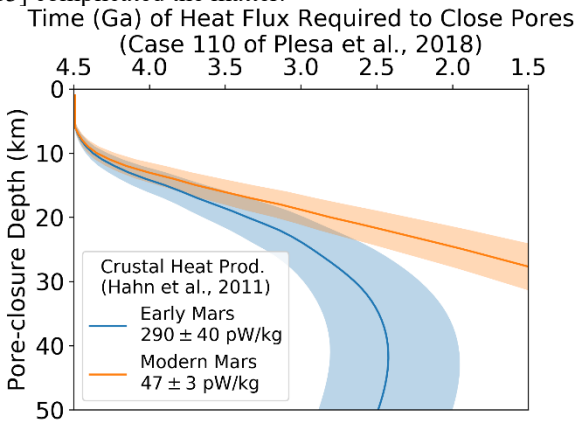

Figure 1: We calculated heat flux required to close porosity at a given depth (y-axis) into the Martian crust [11]. We used [10] to calculate historic heat flux at InSight's landing site, where case 110 assumed a very hot early Mars. This provides the latest time Mars was hot enough to close porosity (x-axis) at a given depth. We assumed crustal heat production from either ancient or modern Mars [9] as endmembers. Further, we assumed the rheology of wet diabase and a thermal conductivity of 1.5 W/m/K but considered other possibilities in [11].

Potential origin of crustal layering: We consider three potential origins for the crustal layers of Mars.

Cementation by aquifer. In this case, the 22-km-deep transition is formed first by a pore closure event. As suggested by [13], an aquifer may have partially closed pores in the 8.5-22 km layer by cementation, forming the shallower 8.5-km-deep transition. However, <2% of the pore space in this second layer could be cement [7], which may not fully explain the difference in porosity between the upper two layers.

Later emplacement of upper layer. Here, we assume that a pore closure event created a transition at 13.5 km. Only later was an 8.5 km layer emplaced atop the crust from some combination of volcanism, sediment, and

impact ejecta. A similar scenario is suggested by [6]. Following Figure 1, pore closure at 13.5±3 km depth would occur $4.1^{+0.3}_{-0.7}$ Ga (or earlier), where uncertainty stems from uncertainties in both the transition depth and the heat flux necessary for pore closure at that depth. As with [11], this roughly aligns with the timing of large-basin-forming impacts as is plausible.

Pore generation by impacts. Our last possibility was also posited by [7, 13]. Here, the shallower 8.5 km transition formed first by viscous pore closure. Subsequently, impacts could generate new porosity by fracturing the deeper crust. Afterward, a second pore closure event could form the deeper 22 km transition. Porosity would close at 8.5±1.5 km depth $4.43^{+0.06}_{-0.16}$ Ga—very early in Martian history. Later pore closure at 22±3 km depth could occur as early as 3.7 Ga or as late as 1.3 Ga depending on the assumed crustal heat production. This leaves a 0.6-3 Gyr gap when impacts can occur between pore closure events. Because both these last scenarios are plausible, we investigated how well impacts could generate porosity.

Impact-induced Tensile Fragmentation: After an impact, a compressive shock front passes through the rock, followed shortly by a tensile dilational wave. As a rock's tensile strength tends to be lower than its compressive strength, rock is more easily fractured with tension. The extent of pore generation by in-situ impact fracturing (i.e. not crater ejecta deposits) has been explored using scaling laws [e.g. 14-16] and, more recently, hydrocode simulations [e.g. 8, 17]. Put simply, the peak tensile stress of an impact decays with distance:

$$\text{stress} \propto \left(\frac{\text{distance}}{\text{impactor radius}}\right)^{a+b\times(\text{impactor speed [km]})}$$

where a and b are constants. This tensile stress must overcome both overburden pressure and a rock's tensile strength to fracture it.

Values for a and b were provided by [14, 15], but results vary greatly depending on which study is used [18]. However, recent simulation results [17] provide the size of the hemispheric tensile fragmentation zone following a 1-km-diameter impactor hitting the Moon at three velocities. We use these data to fit for a and b, allowing us to use our scaling law to estimate the extent of pore generation from an impact. Our simple equation approximately agrees with simulation results for even larger impacts by [17]. We therefore investigate if known craters around InSight can generate porosity 8.5-22 km deep (Figure 2).

The craters nearest InSight are small—the impacts that formed them would only generate shallow porosity. Meanwhile, larger craters are too distant for associated impacts to have generated significant porosity beneath InSight's landing site. Thus, in-situ impact-induced fragmentation could not explain InSight's observed crustal porosity structure.

Future Work: One possibility is a crater from an impact large enough to generate deep porosity has since been buried [e.g. 21]. Perhaps more likely, pores closed at 13.5 km depth, followed by the later emplacement of 8.5 km of material that now forms Mars' upper crust. This would agree with findings by [22, 23] that, while a discontinuity at ~20 km depth may be global, the upper 8.5 km of crust below InSight is only a local feature.

We plan to refine our estimates of potential pore closure event timings with updated thermal models [24] and the extent of in-situ impact fracturing with iSALE simulations [e.g. 17]. We will search for global trends in porosity stratification with a Monte Carlo model [25] updated with our fracturing results and crater ejecta.

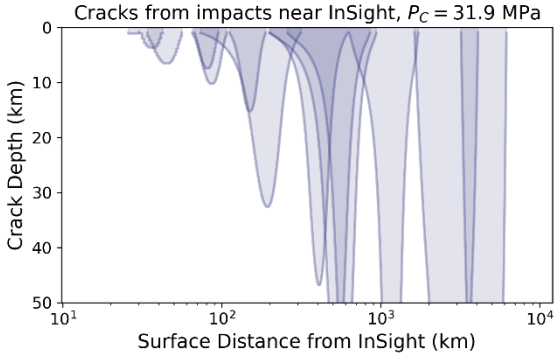

Figure 2: For a set of craters, we calculate the extent of porosity generated from its respective impact as a function of distance from InSight. We reduced computation time by only using craters in a catalog [19] that were each larger than any other crater closer to InSight than itself. We assumed a 10 km/s impact velocity for each crater to estimate the impactor's size [20] and the extent of generated porosity.

References: [1] Lognonné et al. (2020), *Nat. Geosci. 13*. [2] Knapmeyer-Endrun et al. (2021), *Science 373*(6553). [3] Kim et al. (2021), *JGR: Planets 126*(11). [4] Durán et al. (2022), *Phys. of the Earth & Planet. Int. 325*. [5] Joshi et al. (preprint). [6] Wieczorek et al. (2022), *JGR: Planets 127*(5). [7] Kilburn et al. (2022), *JGR: Planets 127*(12). [8] Wiggins et al. (2022), *Nat. Comm. 13*. [9] Hahn et al. (2011), *GRL 38*(14). [10] Plesa et al. (2018), *GRL 45*(22). [11] Gyalay et al. (2020), *GRL 47*(16). [12] Wieczorek et al. (2013), *Science 339*(6120). [13] Manga & Wright (2021), *GRL 48*(8). [14] Ahrens & O'Keefe (1987), *Int. J. of Impact Eng. 5*(1-4). [15] Pierazzo et al. (1997), *Icarus 127*(2). [16] Ai & Ahrens (2004), *Meteoritics & Planet. Sci. 39*(2). [17] Wiggins et al. (2019), *JGR: Planets 124*(4). [18] Gyalay et al. (2022), *53rd LPSC*, Abs. 1633. [19] Salamunićcar et al. (2012), *Planet. & Space Sci. 60*(1). [20] Holsapple & Housen (2006), *Icarus 191*(2). [21] Frey (2006), *JGR: Planets 111*(E8). [22] Kim et al. (2022), *Science 378*(6618). [23] Li et al. (2022), *Nat. Comm. 13*. [24] Plesa et al. (2023), *54th LPSC*, Abs. 2212. [25] Richardson (2004), *Icarus 204*(2).